

Learning Dirac Spectral Transforms for Topological Signals

Leonardo Di Nino^{1,3}, Tiziana Cattai¹, Sergio Barbarossa¹, Ginestra Bianconi² and Paolo Di Lorenzo^{1,3}

¹Dept. of Information Engineering, Electronics, and Telecommunications, Sapienza University of Rome, Italy

²School of Mathematical Sciences, Queen Mary University of London, UK.

³Consorzio Nazionale Interuniversitario per le Telecomunicazioni, Parma, Italy

Email: {leonardo.dinino, tiziana.cattai, sergio.barbarossa, paolo.dilorenzo}@uniroma1.it, g.bianconi@qmul.ac.uk

Abstract—The Dirac operator provides a unified framework for processing signals defined over different order topological domains, such as node and edge signals. Its eigenmodes define a spectral representation that inherently captures cross-domain interactions, in contrast to conventional Hodge–Laplacian eigenmodes that operate within a single topological dimension. In this paper, we compare the two alternatives in terms of the distortion/sparsity trade-off and we show how an overcomplete basis built concatenating the two dictionaries can provide better performance with respect to each approach. Then, we propose a parameterized nonredundant transform whose eigenmodes incorporate a mode-specific mass parameter that captures the interplay between node and edge modes. Interestingly, we show that learning the mass parameters from data makes the proposed transform able to achieve the best distortion-sparsity tradeoff with respect to both complete and overcomplete bases.

Keywords—Graph Signal Processing, Dirac operator of networks, data-driven transform learning, topological signals.

I. INTRODUCTION

Over the years, much interest has grown around the development of algorithms for processing and learning from signals defined over the nodes of a network. The whole machinery of Graph Signal Processing (GSP) [1] revolves mainly around Laplacian operators [2] as key enablers for spectral and convolutional methods based on the localization properties of the Graph Fourier Transform. Also, when moving to higher order topological structures to process edge signals, Hodge-Laplacians are still the cornerstone for both linear [3], [4] and deep neural methods [5]. However, Laplacian operators inherently treat signals within a single topological dimension at a time. In contrast, the Dirac operator of networks [6], [7] naturally couples multiple topological domains, enabling the joint processing of information across different orders. This property makes the Dirac operator particularly appealing for studying network dynamics [8], [9], improving topological data analysis [10], designing neural architectures [11], [12], and modeling systems where different domains are intrinsically entangled by physical principles, such as molecular representation [13].

Algorithms and methods derived from the Dirac equation have demonstrated remarkable performance in processing tasks.

This work was supported by the European Union under the Italian National Recovery and Resilience Plan (NRRP) of NextGenerationEU, partnership on “Telecommunications of the Future” (PE00000001 - program “RESTART”), and by the Horizon SNS JU project 6G-GOALS under grant no. 101139232.

In particular, building on its constitutive properties, it allows to design filtering methods for topological signals, generalizing Tikhonov-like approaches to signals localized around a principal Dirac eigenmode [14] or by recursively capturing subsequently the main contributions aligned to multiple modes [15]. However, to date, it remains unclear under which structural and signal-dependent conditions Laplacian or Dirac bases are more appropriate for processing graph and topological signals, including tasks such as representation, filtering, or sampling. While Laplacian operators provide dimension-wise smooth decompositions, the Dirac operator captures cross-dimensional differential couplings; however, real-world signals may only partially adhere to either model. As a result, the trade-off between spectral localization, sparsity, and topological entanglement in graph signals is not yet fully understood.

Contributions. In this work, we address the aforementioned gap by systematically investigating the conditions under which Dirac-based representations offer advantages over Laplacian ones. Specifically, the main contribution of this work is three-fold: (i) we provide a systematic study of spectral localization properties for joint node-edge signals on networks, clarifying the trade-offs between sparsity, smoothness, and cross-domain coupling; (ii) we construct an overcomplete Laplacian–Dirac frame that allows for the joint analysis of topological signals, providing enhanced flexibility in representation and mode selection; (iii) we introduce an adaptive spectral transform that generalizes both Laplacian- and Dirac-based signal processing, together with a data-driven framework to infer it from observations; the proposed transform learns a sparse mixture of Dirac operators with varying mass parameters, enabling adaptive coupling across topological domains. Numerical experiments on synthetic and real-world datasets confirm the effectiveness of the proposed framework, highlighting its competitiveness with respect to standard Dirac- and Laplacian-based approaches.

II. BACKGROUND

We consider a graph $\mathcal{G}(\mathcal{V}, \mathcal{E})$ consisting of $|\mathcal{V}| = V$ nodes and $|\mathcal{E}| = E$ edges. We consider node signals $\mathbf{x}_0 \in \mathcal{C}^0 \cong \mathbb{R}^V$ and edge signals $\mathbf{x}_1 \in \mathcal{C}^1 \cong \mathbb{R}^E$ as vectors defined over the respective domains. Then, we define a *topological spinor* \mathbf{s} as the composite vector [7]:

$$\mathbf{s} = \begin{pmatrix} \mathbf{x}_0 \\ \mathbf{x}_1 \end{pmatrix} \in \mathcal{C}^0 \oplus \mathcal{C}^1 \cong \mathbb{R}^{V+E}. \quad (1)$$

We relate the two domains via the *discrete gradient* $\delta : \mathcal{C}^0 \rightarrow \mathcal{C}^1$ and the *discrete divergence* $\delta^* : \mathcal{C}^1 \rightarrow \mathcal{C}^0$, each acting element wise as:

$$(\delta \mathbf{x}_0)_e = \mathbf{x}_0[v] - \mathbf{x}_0[u], \quad \forall e : u \trianglelefteq e \trianglerighteq v \quad (2)$$

$$(\delta^* \mathbf{x}_1)_v = - \sum_{e: v \trianglelefteq e} \mathbf{x}_1[e] + \sum_{e: v \trianglerighteq e} \mathbf{x}_1[e], \quad \forall v \in \mathcal{V}. \quad (3)$$

where by $\trianglelefteq, \trianglerighteq$ we denote oriented incidence relations between node and edges. These two operators play a central role in discrete calculus [16] and can be represented by the incidence matrix \mathbf{B} , defined entry-wise as $\mathbf{B}[n, e] = 1$ for $n \trianglerighteq e$, $\mathbf{B}[n, e] = -1$ for $n \trianglelefteq e$, and 0 elsewhere. We can rewrite the previous operations as $\delta \mathbf{x}_0 = \mathbf{B}^\top \mathbf{x}_0$ and $\delta^* \mathbf{x}_1 = \mathbf{B} \mathbf{x}_1$. By composing these operators, we obtain different order Laplacian matrices. In particular, the *divergence of the gradient* yields the graph Laplacian \mathbf{L}_0 :

$$\mathbf{L}_0 : \mathcal{C}^0 \rightarrow \mathcal{C}^0 := \mathbf{L}_0 \mathbf{x}_0 = \mathbf{B} \mathbf{B}^\top \mathbf{x}_0. \quad (4)$$

On the contrary, the *gradient of the divergence* yields the 1-Hodge Laplacian \mathbf{L}_1 :

$$\mathbf{L}_1 : \mathcal{C}^1 \rightarrow \mathcal{C}^1 := \mathbf{L}_1 \mathbf{x}_1 = \mathbf{B}^\top \mathbf{B} \mathbf{x}_1. \quad (5)$$

It is well known that the spectral characterization of the Laplacian operators reveals topological insights on the networks [17], enabling domain-aware processing of topological signals via both spectral methods and vertex-localized ones [18]. Clearly, each operator enables processing on a single domain at a time, while the underlying constitutive relation that defines them suggests the possibility of joint representation and learning across contiguous domains.

In this perspective, the Dirac operator of networks has been introduced to simultaneously account for the cross-talking embedded in the differential relations (2)-(3) [7], [14], [15]. The operator $\mathbf{D} : \mathcal{C}^0 \oplus \mathcal{C}^1 \rightarrow \mathcal{C}^0 \oplus \mathcal{C}^1$ acts on the space of topological spinors by mapping one domain into the other:

$$\mathbf{D}\mathbf{s} = \begin{pmatrix} \mathbf{0} & \mathbf{B} \\ \mathbf{B}^\top & \mathbf{0} \end{pmatrix} \begin{pmatrix} \mathbf{x}_0 \\ \mathbf{x}_1 \end{pmatrix} = \begin{pmatrix} \mathbf{B}\mathbf{x}_1 \\ \mathbf{B}^\top \mathbf{x}_0 \end{pmatrix}. \quad (6)$$

The constitutive property of the Dirac operator is that its iterated application is equivalent to the Gauss-Bonnet Laplacian operator \mathbf{L}_G (a.k.a. the super Laplacian), which in matrix form reads as:

$$\mathbf{L}_G \mathbf{s} = \mathbf{D}^2 \mathbf{s} = \begin{pmatrix} \mathbf{B} \mathbf{B}^\top & \mathbf{0} \\ \mathbf{0} & \mathbf{B}^\top \mathbf{B} \end{pmatrix} \begin{pmatrix} \mathbf{x}_0 \\ \mathbf{x}_1 \end{pmatrix} = \begin{pmatrix} \mathbf{L}_0 \mathbf{x}_0 \\ \mathbf{L}_1 \mathbf{x}_1 \end{pmatrix}. \quad (7)$$

Both operators \mathbf{D} and \mathbf{L}_G are self-adjoint with respect to the canonical inner product; hence, their eigenbases form complete orthonormal bases for the space of topological spinors, thereby inducing Fourier-like spectral representations for such signals. In particular, let \mathbf{U} (respectively, \mathbf{U}_H) denote the matrix whose columns are the left singular vectors of \mathbf{B} associated with its nonzero (respectively, zero) singular values. Similarly, we denote by \mathbf{V} (respectively, \mathbf{V}_H) the matrix whose columns are the right singular vectors of \mathbf{B} associated with its nonzero (respectively, zero) singular values. Under this decomposition, the Dirac operator exhibits the following eigenstructure [7]:

$$\mathbf{D} = \Phi \Gamma \Phi^\top \quad (8)$$

where

$$\Phi = \begin{pmatrix} \mathbf{U} & \mathbf{0} & \mathbf{U}_H & \mathbf{U} \\ -\mathbf{V} & \mathbf{V}_H & \mathbf{0} & \mathbf{V} \end{pmatrix} \quad (9)$$

$$\Gamma = \text{blkdiag}\left(-\Sigma, \mathbf{0}_{\xi_1}, \mathbf{0}_{\xi_0}, \Sigma\right) \quad (10)$$

where Σ is the diagonal matrix whose diagonal entries are the nonnull singular values of \mathbf{B} , $\xi_0 = \dim(\ker(\mathbf{B}))$ and $\xi_1 = \dim(\ker(\mathbf{B}^\top))$, respectively. Similarly, the super-Laplacian operator, admits the eigendecomposition:

$$\mathbf{L}_G = \Theta \Lambda \Theta^\top \quad (11)$$

where

$$\Theta = \begin{pmatrix} \mathbf{U}_H & 0 & \mathbf{U} & 0 \\ 0 & \mathbf{V}_H & 0 & \mathbf{V} \end{pmatrix} \quad (12)$$

$$\Lambda = \text{blkdiag}\left(\mathbf{0}_{\xi_0}, \mathbf{0}_{\xi_1}, \Sigma^2, \Sigma^2\right). \quad (13)$$

III. REPRESENTATION OF TOPOLOGICAL SIGNALS VIA DIRAC-LAPLACIAN FRAMES

Comparing the eigendecompositions of the Dirac or Laplacian operators, we can see that the Dirac operator is more suitable to represent spinors whose node and edge components are strictly coupled along the same modes, while the reverse is true for the Laplacian operator. In the general case, where signals might show *spectrally coupled* components as well as *domain-specific* patterns, either the two bases would be sub-optimal in compressed representations. This suggests that in the general case it might be advisable to use a redundant frame, obtained by concatenating the Dirac and Laplacian eigenmodes, and then use a sparsity-enforcing representation, to extract the most meaningful components from both dictionaries.

Proposition 1 (Dirac–Laplacian frame). *Let Φ and Θ denote the orthonormal eigenbases of the Dirac operator and of the super-Laplacian operator, respectively, and define the dictionary*

$$\mathbf{F} = (\Phi \mid \Theta) \in \mathbb{R}^{(V+E) \times 2(V+E)}.$$

Then \mathbf{F} is a tight frame with frame bound $A = 2$, i.e., $\mathbf{F}\mathbf{F}^\top = 2\mathbf{I}_{V+E}$. Consequently, every spinor $\mathbf{s} \in \mathbb{R}^{V+E}$ satisfies the Parseval-type reconstruction formula

$$\mathbf{s} = \frac{1}{2} \sum_{i=1}^{2(V+E)} \langle \mathbf{f}_i, \mathbf{s} \rangle \mathbf{f}_i,$$

where \mathbf{f}_i denotes the i -th column of \mathbf{F} .

While such a dictionary offers a well-posed representation framework, it remains limited to signals exhibiting either perfect compatibility or perfect incompatibility between the two domains at a given scale. To handle signals that may be entangled at different relative scales, we need to develop more refined analytical tools, as illustrated in the next section.

IV. LEARNING DIRAC SPECTRAL TRANSFORMS

In this section, we first introduce a principled framework to build a spectral transform from mixtures of Dirac equations. We then leverage the proposed approach to formulate a learning problem that finds an optimal transform in a data-driven manner.

A. Dirac equation of networks

The Dirac equation on networks [7] has been introduced for signal processing tasks to account for the relative scaling between topological modes, thereby enabling intermediate regimes between coupled and uncoupled dynamics [15]. It builds on the eigenstates of the topological wave equation:

$$i\partial_t \mathbf{s} - \mathcal{H}\mathbf{s} = 0, \quad (14)$$

where i denotes the imaginary unit, $\mathcal{H} = \mathbf{D} + m \begin{pmatrix} \mathbf{I}_V & \mathbf{0} \\ \mathbf{0} & -\mathbf{I}_E \end{pmatrix}$ and $m \geq 0$ parametrizes the *mass* [19].

The eigenstates ψ of \mathcal{H} , satisfying the equation $\mathcal{H}\psi = E\psi$, can be shown to exhibit the following structure for each nonzero graph frequency λ_i [15]:

$$\psi_i^- = \zeta^- \begin{pmatrix} \frac{\lambda_i}{|E|+m} \mathbf{u}_i \\ -\mathbf{v}_i \end{pmatrix}, \quad \psi_i^+ = \zeta^+ \begin{pmatrix} \mathbf{u}_i \\ \frac{\lambda_i}{|E|+m} \mathbf{v}_i \end{pmatrix}, \quad (15)$$

where ζ^\pm are constants used to have unit norm vectors. The harmonic eigenvectors are invariants to this new parametrization and associated to energies equal in absolute value to the mass.

B. Spectral Transform based on mixtures of Dirac equations

Inspired by the structure of the eigenstates of the Dirac equation of networks in (15), we propose a Fourier-like transform $\mathcal{T}_{\mathbf{D},\mathbf{m}}$ that incorporates a mode-dependent mass contribution across the natural modes of the Dirac operator. Specifically, let $\mathbf{m} = [m_1, \dots, m_r]^\top \in \mathbb{R}_+^r$ be a vector of mass parameters, where $r = V + E - (\xi_0 + \xi_1)$, since the harmonic subspace spanned by Ψ_H is invariant under mass parameterization. Following the notation as in (15), we define a mass-parameterized Fourier operator built as $\bar{\Psi}(\mathbf{m}) = (\Psi^-(\mathbf{m}^-) \mid \Psi_H \mid \Psi^+(\mathbf{m}^+))$, where the i -th column ψ_i of $\bar{\Psi}(\mathbf{m})$ is built as in (15), but with a mode-specific mass parameter m_i . Then, the proposed transform $\mathcal{T}_{\mathbf{D},\mathbf{m}} : \mathcal{C}^0 \oplus \mathcal{C}^1 \rightarrow \mathbb{R}^{V+E}$ and its inverse $\mathcal{T}_{\mathbf{D},\mathbf{m}}^{-1} : \mathbb{R}^{V+E} \rightarrow \mathcal{C}^0 \oplus \mathcal{C}^1$ read as:

$$\mathcal{T}_{\mathbf{D},\mathbf{m}}(\mathbf{s}) = \bar{\Psi}(\mathbf{m})^\top \mathbf{s}, \quad (16)$$

$$\mathcal{T}_{\mathbf{D},\mathbf{m}}^{-1}(\hat{\mathbf{s}}) = \bar{\Psi}(\mathbf{m}) \hat{\mathbf{s}}. \quad (17)$$

Intuitively, this transform is parametrized to encode, for each mode, the different degrees of coupling between the node and edge modes, and it relies on the fact that the mass-induced scaling in (15) preserves orthogonality. It defines a complete orthonormal basis for spinors, which includes the Dirac and Laplacian eigenbases as the limiting regimes.

C. Dirac-driven transform learning from signals

In the sequel, we propose an effective algorithm to learn an orthogonal transform in a data-driven fashion. Building on the Dirac-based transform introduced above, we formulate a learning framework to jointly estimate the mode-specific mass parameters, which govern node–edge coupling, and enforce sparsity in the signal representation. We refer to the proposed framework as *Dirac-driven transform learning* (DDTL).

We postulate the following signal model:

$$\mathbf{s} = \sum_{i \in \mathcal{I}} \omega_i \bar{\psi}_i(m_i) + \mathbf{w}, \quad (18)$$

where \mathcal{I} denotes the set of spectral indices supporting a sparse representation of the signal, $\{\omega_i\}_{i \in \mathcal{I}}$ are the expansion coefficients, and \mathbf{w} is a zero-mean white Gaussian noise vector with covariance matrix $\sigma^2 \mathbf{I}_{V+E}$. Then, let us assume to collect T topological spinors arranged in the data matrix $\mathbf{S} = [\mathbf{s}_1, \dots, \mathbf{s}_T]$, and denote by $\Omega = [\omega_1, \dots, \omega_T]$ their corresponding coefficient vectors in the parametrized basis to be learned. Under the model in (18), the maximum likelihood estimator yields the following least-squares problem:

$$\min_{\mathbf{m}, \Omega} \|\mathbf{S} - \bar{\Psi}(\mathbf{m})\Omega\|_F^2. \quad (19)$$

Since the mass parameters affect the scaling of the eigenmodes in a nonlinear manner, we adopt a reparametrization strategy: Instead of learning the mass parameter m_i directly, we learn its induced scaling factor, defined as $k_i = \frac{\lambda_i}{|E_i|+m_i}$, for all $i = 1, \dots, r$, which enters the model linearly. Under this reparametrization, the resulting objective function becomes biconvex in the variables $\mathbf{k} = [k_1, \dots, k_r]^\top$ and Ω . To promote group sparsity in the representation coefficients, we restrict the feasible set of codes to $\mathcal{B}_{\eta_0} := \{\Omega : \|\Omega\|_{2,0} = \eta_0\}$, i.e., the set of matrices with exactly η_0 nonzero rows. Furthermore, to prevent scale ambiguities related to the nonlinear effect of the mass that may interfere with the localization properties of the learned modes, we constrain the columns of $\bar{\Psi}(\mathbf{m})$ to be normalized. This is equivalent to imposing $\bar{\Psi}(\mathbf{m}) \in \text{Ob}(V+E, V+E)$, where $\text{Ob}(V+E, V+E)$ denotes the oblique manifold, i.e., the set of matrices with unit-norm columns. We transfer these structural constraints to auxiliary variables \mathbf{P}, \mathbf{X} , ensuring solutions with desired structures decoupling them from the block-wise convexity of the learning problem. By additionally defining a feasible set for \mathbf{k} , we finally obtain the following optimization problem, where $\eta_0 \in \mathbb{N}$ and $c_1, c_2 \in [0, 1]$ act as tunable hyperparameters:

$$\begin{aligned} \min_{\mathbf{k}, \Omega, \mathbf{P}, \mathbf{X}} \quad & \|\mathbf{S} - \bar{\Psi}(\mathbf{k})\Omega\|_F^2 \\ \text{s.t.} \quad & -c_2 \mathbf{1} \leq \mathbf{k} \leq c_1 \mathbf{1} \\ & \mathbf{X} \in \mathcal{B}_{\eta_0} \\ & \mathbf{P} \in \text{Ob}(V+E, V+E) \\ & \mathbf{P} - \bar{\Psi}(\mathbf{k}) = \mathbf{0} \\ & \mathbf{X} - \Omega = \mathbf{0} \end{aligned} \quad (\text{P1})$$

To solve (P1), we resort to the alternating direction method of multipliers (ADMM) [20], based on the constrained minimization of the augmented Lagrangian. To this end, we introduce two matrix Lagrange multipliers \mathbf{H} and \mathbf{M} , yielding

$$\begin{aligned} \mathcal{L} = \|\mathbf{S} - \bar{\Psi}(\mathbf{k})\Omega\|_F^2 + \frac{\rho_1}{2} \|\bar{\Psi}(\mathbf{k}) - \mathbf{P} + \mathbf{H}\|_F^2 \\ + \frac{\rho_2}{2} \|\Omega - \mathbf{X} + \mathbf{M}\|_F^2. \end{aligned} \quad (20)$$

Combining the feasibility constraints defined in (P1) with the augmented Lagrangian formulation above leads to the following

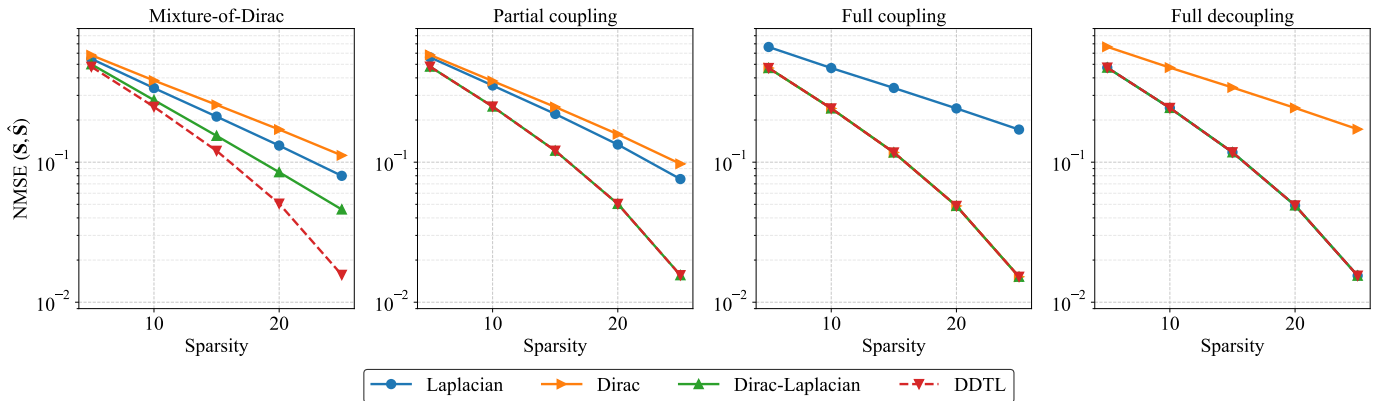


Figure 1: Synthetic results for sparsity-reconstruction trade-off with different classes of signals on different basis

iterative updates¹:

$$\begin{aligned}
 \mathbf{k}^{t+1} &= \underset{-c_2 \mathbf{1} \leq \mathbf{k} \leq c_1 \mathbf{1}}{\operatorname{argmin}} \|\mathbf{S} - \bar{\Psi}(\mathbf{k})\Omega\|_{\mathbf{F}}^2 + \frac{\rho_1}{2} \|\bar{\Psi}(\mathbf{k}) - \mathbf{P} + \mathbf{H}\|_{\mathbf{F}}^2 \\
 \Omega^{t+1} &= \operatorname{diag}\left(\left\{\frac{1}{\|\bar{\Psi}_i(k_i)\|_2^2 + \rho_2}\right\}_i\right) [\rho_2(\mathbf{X} - \mathbf{M}) + \bar{\Psi}^\top(\mathbf{k})\mathbf{S}] \\
 \mathbf{P}^{t+1} &= \mathcal{R}_{\mathcal{O}b}\left\{\mathbf{H} + \bar{\Psi}(\mathbf{k})\right\} \\
 \mathbf{X}^{t+1} &= \mathcal{R}_{\mathcal{B}_{\eta_0}}\left\{\Omega + \mathbf{M}\right\} \\
 \mathbf{H}^{t+1} &= \mathbf{H} + [\bar{\Psi}(\mathbf{k}) - \mathbf{P}] \\
 \mathbf{M}^{t+1} &= \mathbf{M} + (\Omega - \mathbf{X})
 \end{aligned}$$

The retractions $\mathcal{R}_{\mathcal{O}b}$ and $\mathcal{R}_{\mathcal{B}_{\eta_0}}$ are implemented, respectively, by normalizing the columns of the argument matrix [21], and by retaining only the η_0 rows with largest ℓ_2 norm (i.e., highest energy) while setting all remaining rows to zero [22]. The update step with respect to \mathbf{k} instead amounts to a convex optimization problem, which can be solved efficiently using standard numerical methods for quadratic programming. The convergence of the algorithm is monitored using standard arguments from [20]. In practice, the algorithm performs well both with random initialization and in limit-regime initializations as the Dirac and Laplacian eigenbases are.

V. NUMERICAL RESULTS

In the sequel, we assess the performance of the proposed method via numerical experiments on synthetic and real data.

Sparse Representation. With this experiment, we validate the considered representation basis for different classes of signals. We considered instances of Erdős-Rényi random graphs with $V = 40$ nodes and $E = 80$ edges. We consider the following classes of signals all derived by the considered model (18): (i) *fully coupled signals* (Dirac regime), obtained for $m_i = 0, \forall i \in [r]$, (ii) *fully decoupled signals* (Laplacian regime), obtained for $m_i \gg 0, \forall i \in [r]$, (iii) *partially coupled signals* (Dirac-Laplacian regime), obtained for $m_i = 0, \forall i \in [r]$.

¹For notational simplicity, we omit time indices, with the understanding that the scheme proceeds sequentially.

$\mathcal{I}_C, m_j \gg 0, \forall j \in \mathcal{I}_U$ such that $\mathcal{I}_U \cup \mathcal{I}_U = [r]$, (iv) *mixture-of-Dirac signals* where in (18) we define a mass distribution across the modes via a radial basis function with a Cauchy-like kernel. Ideally, coupling should degrade with frequency as high frequency patterns are associated with localized modes. We fix the bandwidth to $\eta_0 = 35$ and assume a shared spectral support during the generation step. In each scenario, we generate $M = 600$ signals with random Gaussian coefficients. Harmonic components are excluded, as they are optimally captured by any of the considered bases. We solve the DDTL problem on the given signals setting $c_1 = c_2 = 1, \rho_1 = \rho_2 = 10$, and then compare the normalized mean squared error (NMSE) between the observed data \mathbf{S} and their reconstructed version $\hat{\mathbf{S}}$, obtained via orthogonal matching pursuit (OMP) [23], across different sparsity levels. The comparison is performed over the considered bases: the Laplacian basis, the Dirac basis, the joint Dirac-Laplacian frame, and the DDTL transform.

In Figure 1, we show the results averaged over 10 realizations of the depicted experimental setting. As expected, we can observe a factor-of-two in bandwidth relation between Dirac and Laplacian representation in the fully coupled and decoupled signals, with the frame achieving optimal sparsity-reconstruction trade-off in the two scenarios and in the partially coupled one. The proposed data-driven transform not only achieves optimal representation performance in these three scenarios, but also exhibits a significant gain in more challenging settings (i.e., mixture-of-Dirac signals), effectively capturing complex cross-domain entanglement patterns that cannot be described by purely Dirac or Laplacian regimes.

Denoising. In this experiment, we evaluate the performance of our proposed method in a denoising task, to assess the impact of noise on the learning algorithm. We consider topological signals naturally entangled as quantities measured in the context of water distribution networks (WDNs), where node and edge signals represent, respectively, pressure and flow data. This induces a challenging model mismatch as the signals cannot be supposed to be modeled with a perfectly finite bandwidth. We consider the Anytown network, consisting of $V = 22$ nodes and $E = 41$ edges, retrieving the first $T = 240$ node pressure measurements and pipe flow-rates signals as collected in [24].

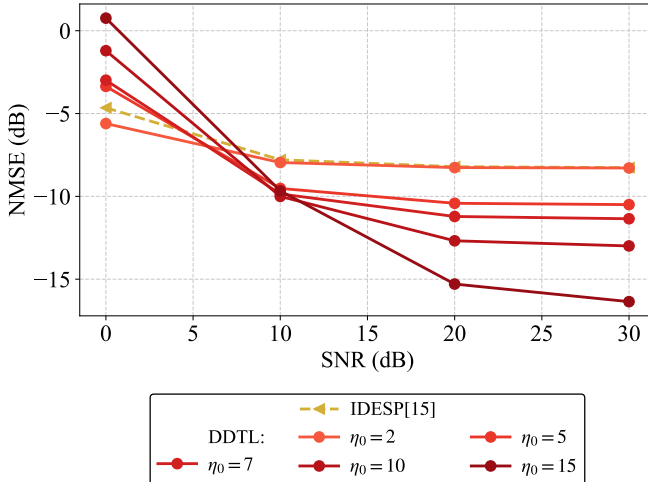


Figure 2: NMSE vs. SNR, for different algorithms.

We thus have a ground truth data matrix \mathbf{S} that we corrupt with AWGN, at various signal-to-noise ratio (SNR) levels. The proposed DDTL problem is solved for different bandwidths, considering the solution as the optimal filtered signal to be $\Psi(\mathbf{k}^*)\Omega^* \approx \mathbf{S}$. We compare the performance of the algorithm with the iterative filtering framework (IDESP) proposed in [15]. The results are reported in Fig. 2, which depicts the NMSE between the ground-truth and filtered signals as a function of SNR, averaged over 10 independent noise realizations. The bandwidth plays a crucial role in noise robustness. For small bandwidth values, the proposed method slightly outperforms IDESP at low SNR levels, whereas increasing the bandwidth as the SNR improves yields progressively larger performance gains. These results demonstrate the capability of the proposed model to learn an informative basis for representing structured signals even under mild modeling assumptions. On the other hand, the algorithm relies on data-driven learning, whereas IDESP constitutes a fully analytical alternative.

VI. CONCLUSIONS

In this paper, we proposed a learnable spectral transform for the representation of topological signals jointly defined on nodes and edges to overcome the limitations of fixed representations. We introduced a parametric Dirac-based transform with mode-dependent mass parameters, enabling a continuous interpolation between coupled and decoupled regimes. We then formulated a Dirac-Driven Transform Learning (DDTL) framework to learn these parameters from data under sparsity constraints. Numerical results on synthetic and real-world datasets demonstrated improved sparsity–distortion trade-offs and competitive denoising performance compared to Laplacian-, Dirac-, and frame-based representations. Future work will investigate extensions to higher-order structures and integration within learning-based architectures for topological signal processing.

REFERENCES

- [1] A. Sandryhaila and J.M.F. Moura, “Discrete Signal Processing on Graphs,” *IEEE Transactions on Signal Processing*, vol. 61, no. 7, pp. 1644–1656, 2013.
- [2] A.J. Smola and R. Kondor, “Kernels and Regularization on Graphs,” in *16th Annual Conference on Learning Theory and 7th Kernel Workshop, COLT/Kernel 2003, Washington, DC, USA*. Springer, 2003, pp. 144–158.
- [3] S. Barbarossa and S. Sardellitti, “Topological signal processing over simplicial complexes,” *IEEE Transactions on Signal Processing*, vol. 68, pp. 2992–3007, 2020.
- [4] E. Isufi, G. Leus, B. Beferull-Lozano, S. Barbarossa, and P. Di Lorenzo, “Topological signal processing and learning: Recent advances and future challenges,” *Signal Processing*, p. 109930, 2025.
- [5] M. Yang, E. Isufi, and G. Leus, “Simplicial convolutional neural networks,” in *IEEE International Conference on Acoustics, Speech and Signal Processing*. IEEE, 2022, pp. 8847–8851.
- [6] G. Bianconi, *Higher-order networks*, Cambridge University Press, 2021.
- [7] G. Bianconi, “The topological Dirac equation of networks and simplicial complexes,” *Journal of Physics: Complexity*, vol. 2, no. 3, 2021.
- [8] L. Calmon, S. Krishnagopal, and G. Bianconi, “Local Dirac synchronization on networks,” *Chaos: An Interdisciplinary Journal of Nonlinear Science*, vol. 33, no. 3, 2023.
- [9] T. Carletti, L. Giambagli, R. Muolo, and G. Bianconi, “Global topological Dirac synchronization,” *Journal of Physics: Complexity*, vol. 6, no. 2, pp. 025009, 2025.
- [10] F. Baccini, F. Geraci, and G. Bianconi, “Weighted simplicial complexes and their representation power of higher-order network data and topology,” *PHYSICAL REVIEW E Phys Rev E*, vol. 106, pp. 034319, 2022.
- [11] C. Nauck, R. Gorantla, M. Lindner, K. Schürholz, A.S.J.S. Mey, and F. Hellmann, “Dirac–Bianconi graph neural networks-enabling long-range graph predictions,” in *ICML 2024 Workshop on Geometry-grounded Representation Learning and Generative Modeling*, 2024.
- [12] C. Battiloro, L. Testa, L. Giusti, S. Sardellitti, P. Di Lorenzo, and S. Barbarossa, “Generalized simplicial attention neural networks,” *IEEE Transactions on Signal and Information Processing over Networks*, 2024.
- [13] J. Wee, G. Bianconi, and K. Xia, “Persistent Dirac for molecular representation,” *Scientific Reports*, vol. 13, no. 1, pp. 11183, 2023.
- [14] L. Calmon, M.T. Schaub, and G. Bianconi, “Dirac signal processing of higher-order topological signals,” *New Journal of Physics*, vol. 25, no. 9, pp. 093013, 2023.
- [15] R. Wang, Y. Tian, P. Liò, and G. Bianconi, “Dirac-equation signal processing: Physics boosts topological machine learning,” *PNAS nexus*, vol. 4, no. 5, pp. pgaf139, 2025.
- [16] L.J. Grady and J.R. Polimeni, *Discrete calculus: Applied analysis on graphs for computational science*, vol. 3, Springer, 2010.
- [17] F.R.K. Chung, *Spectral graph theory*, vol. 92, American Mathematical Soc., 1997.
- [18] A. Ortega, *Introduction to graph signal processing*, Cambridge University Press, 2022.
- [19] G. Bianconi, “The mass of simple and higher-order networks,” *Journal of Physics A: Mathematical and Theoretical*, vol. 57, no. 1, 2024.
- [20] S. Boyd, N. Parikh, E. Chu, B. Peleato, J. Eckstein, et al., “Distributed optimization and statistical learning via the alternating direction method of multipliers,” *Foundations and Trends® in Machine learning*, vol. 3, no. 1, pp. 1–122, 2011.
- [21] P.-A. Absil, R. Mahony, and R. Sepulchre, *Optimization algorithms on matrix manifolds*, Princeton University Press, 2008.
- [22] R.G. Baraniuk, V. Cevher, M.F. Duarte, and C. Hegde, “Model-based compressive sensing,” *IEEE Transactions on Information Theory*, vol. 56, no. 4, pp. 1982–2001, 2010.
- [23] J.A. Tropp and A.C. Gilbert, “Signal recovery from random measurements via orthogonal matching pursuit,” *IEEE Transactions on information theory*, vol. 53, no. 12, pp. 4655–4666, 2007.
- [24] A. Tello, H. Truong, A. Lazovik, and V. Degeler, “Large-scale multipurpose benchmark datasets for assessing data-driven deep learning approaches for water distribution networks,” *Engineering Proceedings*, vol. 69, no. 1, pp. 50, 2024.